Fabrication of hyaluronic acid-gold nanoparticles with chitosan to modulate neural differentiation of mesenchymal stem cells

Chiung-Chyi Shen[a,b,c], Meng-Yin Yang[a,c], Kai-Bo Chang[d], Chia-Hsuan Tseng[e], Yi-Ping Yang[f], Yi-Chin Yang[a], Mei-Lang Kung[g], Wei-Yi Lai[f], Tzu-Wei Lin[f], Hsien-Hsu Hsieh[h], Huey-Shan Hung[d,i,*]

[a]Neurological Institute Head of Department of Neurosurgery Taichung Veterans General Hospital, Taichung, Taiwan, ROC; [b]Department of Physical Therapy, Hung Kuang University, Taichung, Taiwan, ROC; [c]Basic Medical Education Center, Central Taiwan University of Science and Technology, Taichung, Taiwan, ROC; [d]Graduate Institute of Biomedical Science, China Medical University, Taichung, Taiwan, ROC; [e]Department of Occupational Safety and Health, China Medical University, Taichung, Taiwan, ROC; [f]Department of Medical Research, Taipei Veterans General Hospital, Taipei, Taiwan, ROC; [g]Department of Medical Education and Research, Kaohsiung Veterans General Hospital, Kaohsiung, Taiwan, ROC; [h]Blood Bank, Taichung Veterans General Hospital, Taichung, Taiwan, ROC; [i]Translational Medicine Research, China Medical University Hospital, Taichung, Taiwan, ROC

Abstract

Background: Chitosan (Chi) is a natural material which has been widely used in neural applications due to possessing better biocompatibility. In this research study, a novel of nanocomposites film based on Chi with hyaluronic acid (HA), combined with varying amounts of gold nanoparticles (AuNPs), was created resulting in pure Chi, Chi-HA, Chi-HA-AuNPs (25 ppm), and Chi-HA-AuNPs (50 ppm).

Methods: This study focused on evaluating their effects on mesenchymal stem cell (MSC) viability, colony formation, and biocompatibility. The surface morphology and chemical position were characterized through UV-visible spectroscopy (UV-Vis), Fourier-transform infrared spectroscopy (FTIR), SEM, and contact-angle assessment.

Results: When seeding MSCs on Chi-HA-AuNPs (50 ppm), the results showed high cell viability, biocompatibility, and the highest colony formation ability. Meanwhile, the evidence showed that Chi-HA-Au nanofilm was able to inhibit nestin and β-tubulin expression of MSCs, as well as inhibit the ability of neurogenic differentiation. Furthermore, the results of matrix metalloproteinase 2/9 (MMP2/9) expression in MSCs were also significantly higher in the Chi-HA-AuNP (50 ppm) group, guiding with angiogenesis and wound healing abilities. In addition, in our rat model, both capsule thickness and collagen deposition were the lowest in Chi-HA-AuNPs (50 ppm).

Conclusion: Thus, in view of the in vitro and in vivo results, Chi-HA-AuNPs (50 ppm) could not only maintain the greatest stemness properties and regulate the neurogenic differentiation ability of MSCs, but was able to also induce the least immune response. Herein, Chi-HA-Au 50 ppm nanofilm holds promise as a suitable material for nerve regeneration engineering.

Keywords: Chitosan; Hyaluronic acid; Mesenchymal stem cells; Nerve regeneration

1. INTRODUCTION

Central nervous system (CNS) disorders such as stroke and spinal cord injury (SCI) are usually caused by loss of function or the death of neurons. Previous studies revealed various potential tools could apply in neural regeneration engineering.[1,2] Regarding neural regeneration, it has been proved that neural stem cells (NSCs) and neural progenitor cells (NPCs) could be employed to restore neuronal functions due to self-renewal and multipotential abilities.[3,4] Literature elucidated NSCs obtained from embryos could differentiate into neurons and glial cells to improve neuronal functions.[5] However, it still required extra addition of bioactive molecules to maintain cell survival and differentiation ability, while transplanting NSCs into the injury area may have risk of tumor development.[6]

Mesenchymal stem cells (MSCs) are considered to be a potential therapeutic tool due to relatively abundant and easy to obtain compared with NSCs or NPCs. MSCs can also promote tissue regeneration and attract stem cell–like progenitor cells (PCs) to differentiate through secreting various growth factors and cytokines.[7] Due to their self-renewal ability and lower likelihood for immune reaction, MSCs would not cause severe immune response after being implanted into foreign host body.[8] Previous research has indicated that MSCs can act as regenerative medicine in Alzheimer's disease model mice.[9] Furthermore, after appropriate induction with several growth factors, MSCs could differentiate into neuronal-related cells.[10]

*Address correspondence. Dr. Huey-Shan Hung, Graduate Institute of Biomedical Science, China Medical University, 91, Hsueh-Shih Road, Taichung 404, Taiwan, ROC. E-mail address: hunghs@mail.cmu.edu.tw (H.-S. Hung).

Conflicts of interest: The authors declare that they have no conflicts of interest related to the subject matter or materials discussed in this article.

Journal of Chinese Medical Association. (2021) 84: 1007-1018.

Received June 24, 2021; accepted July 19, 2021.

doi: 10.1097/JCMA.0000000000000589.

Many biomaterials were employed to develop novel approaches surrounding nerve tissue regeneration. Tissue is a cell composite consisting of cells and extracellular matrices (ECM). In general, scaffolds could provide support as artificial ECM promoting cells to proliferate and maintain differentiation ability. Currently, biomimetic natural biopolymer scaffolds are potential tissue scaffolds due to better biocompatibility when compared with synthetic scaffolds.[11] Chitosan (Chi) is a natural linear polysaccharide and is a deacetylated derivative of chitin. Chi is a biomaterial candidate for nerve tissue engineering due to high biocompatibility and housing of growth factors, which could be used to induce differentiation of NSCs.[12,13] In addition, Chi's remarkable biological properties including bioresorbable degradation products, hydrophilicity, biocompatibility, and strong cellular binding capability can work as unique properties required for tissue engineering, wound healing, and drug delivery approaches.[14,15]

The cell adhesion, proliferation, differentiation, and migration ability could be influenced by artificially designed scaffolds.[16] Therefore, hyaluronic acid (HA) was used to design customized scaffolds. HA is an important constituent of ECM and plays an important role in tissue repair through biocompatibility and biodegradability traits.[17] Indeed, certain research has attempted to combine HA with other biomaterials such as collagen[18] and Chi.[19] HA is also important in the maintenance of joint lubrication through hydration and moisturization of tissues, as well as cell movement and differentiation.[20,21] Further, HA is crucial in biological functions such as water retention capacity, the providing of nutrients, and the removal of waste from cells compared with other natural and synthetic polymers.[22] It is also the preferred filling material, as there is no deformity occurring in its structure and shape at the injected location during clinical treatments.[23]

Nanoparticles (NPs) such as gold and silver have been widely used for biomedical applications.[24] Gold NPs (AuNPs) are highly biocompatible and provide many promising multiangled approaches for tissue regeneration.[25,26] Mentioned in previous studies, nanocomposites of synthetic polyurethane (PU) combined with AuNPs, exhibited better biocompatibility, as well as the least monocyte activation, foreign tissue reaction, and resistance to oxidative degradation.[27,28] Other literature also indicated AuNPs can well interact with various polymers, such as fibronectin and collagen, thus demonstrating better biological performance in differentiation and proliferation capability of stem cells.[29,30]

It is a challenge in maintaining stemness to inhibit MSCs differentiation while being implanted into the injury area. Hence, the Chi-HA-AuNP nanocomposites were created in current research. Through investigating the hydrophilicity, biocompatibility, anti-inflammatory capability, and stemness properties culturing with MSCs in vitro, this study is trying to realize under which concentration of AuNPs there would be greater cell viability, as well as less immune reaction and colony formation. Additionally, capsule thickness and collagen deposition were also observed in vivo. In future studies, researchers hope to improve and conquer the barriers surrounding nerve regeneration engineering.

2. METHODS

2.1. Material preparation

2.1.1. Preparation of Chi

The Chi powder (molecular weight = 510 kDa) was purchased from Sigma-Aldrich (Saint Louis, MO, USA). To prepare Chi substrates, a 1.5% Chi solution was dissolved in 1.5% acetic acid for 12 hours at room temperature. The resulting solution would subsequently be used in the upcoming experiments.

2.1.2. Preparation of Chi-HA–coated AuNp films

The Chi solution previously prepared was then used to synthesize with HA, before being mixed with different concentrations (~25 and ~ 50 ppm) of AuNPs (obtained from Gold Nanotech Inc, Taipei, Taiwan) to form the nanocomposites, Chi-HA-AuNPs. Thus, we had prepared several materials for the experiments: Chi-HA, Chi-HA-Au (25 ppm), and Chi-HA-Au (50 ppm). AuNps were acquired from bulk gold and atomically vaporized through an electrically gasified method under vacuum conditions before being harvested in a cold trap system through a centrifuge.[31] All of the materials were then coated to the cell culture tissue dish, cell culture plate, and a 15-mm round coverslip glass in the amount of 20 μg/cm^2, to form thin films for the upcoming experiments.

2.2. Material characterization

2.2.1. Ultraviolet-visible spectroscopy

The ultraviolet-visible (UV-Vis) spectra of materials were analyzed by a spectrophotometer having a wavelength ranging from 400 to 1000 nm, where the peak at 545 nm was the absorption wavelength of AuNps. The following procedures outline the steps taken to measure the sample: the quartz colorimetric tube was cleaned with deionized water, wiped dry with mirror paper, then added deionized water to the quartz colorimetric tube and measured for background absorption. Next, each sample solution was measured sequentially. Before measuring the different various, the quartz tube had to be repeatedly cleaned with deionized water to remove any residuals from the previous sample, which would affect the precision of the data. Origin Pro 8 (Originlab Corporation, Northampton, MA, USA) software was used to measure and quantify the data.

2.2.2. Fourier transform infrared spectroscopy analysis

The infrared (IR) spectra were obtained by a Fourier transform IR spectrometer. During this part of experiment, we mixed 200 mm from each experimental group, respectively, HA, Chi, Chi-HA, and Chi-HA-Au, with 0.06 g of potassium bromide (KBr, Sigma, Saint Louis, MO, USA), then independently scanned them eight times in the wave range of 400 to 4000 cm^{-1}, coupling with a resolution setting of 2 cm^{-1} to obtain the spectrum.

2.2.3. Scanning electron microscope

In this study, a SEM (JEOL JSM-7800F, Tokyo, Japan) was employed to observe the surface morphology of cells on different materials.[32] The cells (1 × 10^4/mL) were cultured for 48 hours, fixed in a 2.5% glutaraldehyde solution for 8 hours, and dehydrated at a concentration of 30% to 100%, before being dried at a critical point and coated with gold. This type of electron microscope can detect the surface of samples through a focused electron beam. After becoming excited by the electron beam, a secondary electron emitted by atoms of samples could be collected by a secondary electron detector. Afterward, the topography of the surface would be shown as an image.

2.3. Biocompatibility test

2.3.1. Cell culture of Wharton's jelly MSCs and immunophenotyping

MSCs were harvested from human umbilical cord Wharton's jelly tissue, stored in a condition medium (a high glucose Dulbecco's Modified Eagle's Medium [DMEM, Invitrogen, Thermo Fisher Scientific, Inc., Waltham, MA, USA], supplemented with 1% [v/v] antibiotics 100 U/mL penicillin/streptomycin, 1% sodium pyruvate). The collected human umbilical cord tissues were washed three times with Ca^{2+}- and Mg^{2+}-free Dulbecco's phosphate-buffered saline (DPBS; Life Technology, Waltham, MA, USA).

The cells were then cultured in a high glucose DMEM (Gibco, Waltham, MA, USA; 10% fetal bovine serum [FBS], 100 U/mL P/S, 1% sodium pyruvate) for 14 to 18 hours at 37°C in a 95% air/5% CO_2 humidified atmosphere before being removed with 0.05% trypsine-ethylene diamine tetraacetic acid (EDTA).

The cellular morphology became homogenously spindle-shaped in cultures after four to eight passages. The specific surface molecules of cells from the Wharton's jelly were characterized by flow cytometry. Cells were detached with 2 mM EDTA in phosphate-buffered saline (PBS), washed with PBS containing both 2% bovine serum albumin (BSA) and 0.1% sodium azide (Sigma), and then incubated with the respective antibody conjugated with either fluorescein isothiocyanate (FITC) or phycoerythrin (PE) against the indicated markers: CD14-PE, CD29-FITC, CD34-PE, CD44-FITC, CD45-PE, CD90-FITC (BD Pharmingen, CA, USA). PE-conjugated IgG1 and FITC-conjugated IgG1 were used as isotype controls (BD Pharmingen). Therefore, the cells were analyzed through immunofluorescence microscopy and a flow cytometer (LSR II; BD Pharmingen). Cells of the eighth passage maintained the correct phenotype and were used in this research.

2.3.2. Cell viability examination

To test cell viability, we used fluorescent live cell assay. Cells (1×10^4/well) were cultured with 2 μM calcein-acetoxymethyl (AM) for at least 30 minutes under the condition of a regular 95% air/5% CO_2 incubator at 37°C. Calcein-AM is a commonly used green fluorescent cell marker but it is nonfluorescent. Due to the advantage of being membrane-permeant, calcein-AM can enter into cells during incubation. After calcein-AM is hydrolyzed by intracellular esterases, calcein will be produced. Calcein is a hydrophilic, fluorescent compound which is retained in cell cytoplasm. The cell nuclei were stained with 4, 6-diamidino-2-phenylindole (DAPI) (1 μg/mL) for 10 minutes and the results then observed under a fluorescence microscope.

2.3.3. Monocyte activation tests

Monocyte isolation of human blood samples taken from volunteer donors was performed using the culture method. The cells (1×10^5/well) were seeded on a 24-well plate coated with different materials for a 96-hour incubation period at 37°C in 5% CO_2 in a medium of Roswell Park Memorial Institute which contained 10% FBS and 1% (v/v) antibiotic (10,000 U/mL penicillin G and 10 mg/mL streptomycin). The adherent cells were then trypsinized (0.05%) before an inverted phase contrast microscope was used to count the amount of monocytes and macrophages based on their morphology. The ratio between the number of monocytes and macrophages (the conversion ratio) was performed as an inflammatory index.

2.3.4. Colony formation ability of MSCs

Colony formation assay was applied to examine the ability of single cell growth into a colony in vitro, where the colony is defined to be composed of 50 cells.[33] In this study, MSCs on different materials were seeded in the plate to form colonies in 1 to 3 weeks. After 1 to 3 weeks incubating, the colonies were fixed with 6% v/v glutaraldehyde and stained with 0.5% w/v crystal violet, before the number of colonies was counted using a stereomicroscope.

2.3.5. Immunofluorescence staining

In this study, cells were grown in a basal medium as previously described. The expression of nestin and β-tubulin was visualized through immunofluorescence staining. The MSCs (2×10^4 cells in each well) were incubated for 48 hours. The cells were then fixed, permeabilized, and washed with PBS. The primary antibodies (primary anti-CD44 antibody [Santa Cruz, CA, USA]) were added to the culture plate and incubated overnight. Secondary antibodies (FITC-conjugated antibody [green color fluorescence]) were added to the sample for 60 minutes before the cell nuclei were stained with DAPI (1 μg/mL) for 10 minutes.

2.4. Biological functional examination

2.4.1. Gelatin zymography assay

The cells (2×10^5/well) were seeded in a six-well plate and incubated overnight to allow the cells to reach attachment. After incubating for 48 hours, the culture medium was collected. The samples were separated by 10% sodium dodecyl sulfate polyacrylamide gel electrophoresis containing 2% gelatin, and the gel was incubated with a denaturing buffer (40 mM Tris-HCl, pH 8.5, 0.2M NaCl, 10 mM $CaCl_2$, and 2.5% Triton X-100) for 30 minutes at room temperature. The gel was then slowly stirred at room temperature and equilibrated with a development buffer (40 mM Tris-HCl, pH 8.5, 0.2 M NaCl, 10 mM $CaCl_2$, and 0.01% NaN_3) for at least 16 to 18 hours to become activated in a 37°C water bath. Afterward, the gel was stained with 0.2% Coomassie Brilliant Blue R-250 (10% acetic acid and 50% methanol) and washed in a destaining buffer (10% acetic acid, 20% methanol). After Coomassie blue staining, the protease-digested gelatin area appeared as clear bands against a dark blue background. The resulting gel was scanned in a densitometer and matrix metalloproteinase (MMP) gelatinase activity was quantified using Image Pro Plus 5.0 software (Media Cybernetics, Rockville, MD, USA).

2.4.2. Real-time polymerase chain reaction assay

The total amount of RNA in the cells was extracted by Trizo1 (Invitrogen, Thermo Fisher Scientific, Inc.). The method used was preformed according to the manual provided by the manufacturer. Cells (1×10^5/well) were seeded into a 10-cm culture dish after 3, 5, 7, and 10 days of incubation. They were then treated with 1 mL of Trizol for 5 minutes, had their RNA extracted by adding 200 μL chloroform (Sigma) for 15 seconds and then kept for 3 minutes at room temperature before being centrifuged at 12 000 rpm for 15 minutes at 4°C. The supernatant was removed and 500 μL of isopropanol was added at 4°C for 10 minutes. Finally, the samples were centrifuged at 12 000 rpm for 15 minutes at 4°C. The supernatant was removed and washed twice with 1 mL of alcohol (75%). After drying the RNA, 20 μL of diethyl pyrocarbonate-treated H_2O soluble precipitate was added and quantified by reading the absorbance at 260 nm using an enzyme-linked immunosorbent assay reader (Molecular Devices; SpectraMax M2, CA, USA). cDNA synthesis was performed using a RevertAidTM First Strand cDNA DNA Synthesis Kit (Fermentas, Burlington, Canada) following the manufacturer's procedures. First, 2 μL of oligo (dT) 18 primer and random hexamers (1:1) were added to the RNA sample before being put into a gradient polymerase reaction temperature controller at 65°C for 5 minutes. Afterward, the addition of 4 μL of 5× reaction buffer, 1 μL LockTM RNase inhibitor (20 U/mL), 2 μL deoxynucleotide triphosphates Mix (10 mM), and 1 μL of RevertAidTM M-MuLV Reverse Transcriptase (200 U/mL) proceeded, before being reacted at 42°C for 60 minutes. Finally, each sample was carried out at 70°C for 5 minutes to obtain cDNA. The polymerase chain reaction was carried out using the cDNA as a template and a 1Q2 Fast qPCR System with a reaction volume of 10 μL in accordance with the manufacturer's procedures. First, 0.5 μL of primer (0.3 μM) and 5 μL of enzyme were added to the cDNA sample, with the RNA expression then analyzed using the Step OneTM Plus Real-Time Polymerase Chain Reaction (PCR) System.

2.5. Rat subcutaneous implantation

In this study, rats were used to measure in vivo biocompatibility, with approval given by the Animal Care and Use Committee. All

procedures followed their ethical guidelines and were approved by the Animal Care and Use Committee (La-1071565). Female Sprague Dawley rats (2 to 3 months old) were bred to weigh at approximately 300 to 350 g before the experiments were performed. Under local anesthesia, the dorsal skin was incised at 10 mm to implant the different materials. After 1 month, the wound tissue was resected for examination. Our research team investigated the thickness of the fibrous capsule over six sites through the use of commercial software to quantify the average encapsulated fibrotic tissues. The amount of collagen deposition was observed as a blue color using a Masson's trichrome staining kit (Sigma) according to the manufacturer's instructions. The fibrosis tissue area in the sample sections was calculated by using Image J 4.5 version software (Media Gybertics). Results were expressed as mean ± SD (n = 6).

2.6. Statistical analysis

In this study, all of the experiments were independently performed in triplicate to avoid uncertainty. Data for each test (n = 3 to 6) were collected and presented as mean ± SD. The student *t* test and single-factor analysis of variance (ANOVA) methods were used to investigate the differences between groups. For ANOVA, Bonferroni was chosen for posthoc analysis. A p value less than 0.05 was considered statistically significant.

3. RESULTS

3.1. Characterization of materials

Model concept of preparation of Chi-HA-Au nanocomposites (Fig. 1A). In Figure 1B, the peak of UV-Vis absorption showed up at 545 nm after loading different concentrations of AuNps (~25 and 50 ppm) and combining them with HA and Chi-HA. The Fourier-transform infrared spectroscopy (FTIR) results are shown in Figure 1C.

In addition, the surface topography of Chi, Chi-Au 25 ppm, and Chi-Au 50 ppm was investigated through use of a SEM. When the incorporation of AuNps into Chi-HA occurred, the surface morphology of Chi-HA-AuNP significantly changed (Fig. 2A). The hydrophilicity property of materials is significant for cell attachment to the ECM through cell adhesion molecules. The images show that the water contact angle of Chi-HA, Chi-HA-Au (25 ppm), and Chi-HA-Au (50 ppm) were 60.57°, 58.28°, and 52.56°, respectively (Fig. 2B). Additionally, the average contact angle was quantified in Figure 2B(d), where the Chi-HA-Au 50 ppm group had the lowest contact angle degree (~46.9°, $p < 0.05$), when compared with the Chi-HA-Au 25 ppm (~55.2°, $p < 0.05$) and Chi-HA (~65.8°) groups. Therefore, according to the above results, Chi-HA-AuNPs 50 ppm had greater hydrophilicity properties and also facilitated the adhesion ability of MSCs.

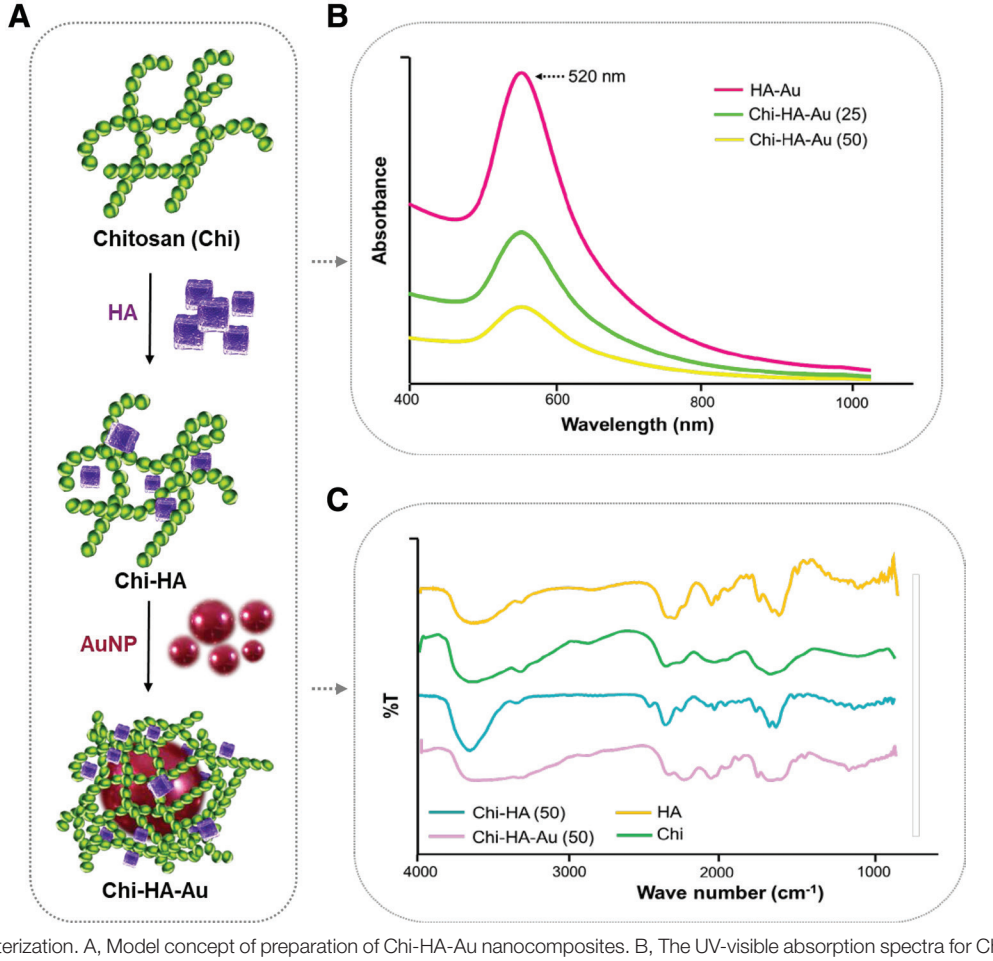

Fig. 1 Material characterization. A, Model concept of preparation of Chi-HA-Au nanocomposites. B, The UV-visible absorption spectra for Chi with HA combined with different concentrations of Au (~25 and 50 ppm). C, FTIR spectra of HA, Chi, Chi-HA, and Chi-HA-Au composites in the total wave number ranges from 400 to 4000 cm^{-1}. All results are representative of one of three independent experiments. Au = gold; Chi = chitosan; FTIR = Fourier-transform infrared spectroscopy; HA = hyaluronic acid; Np = nanoparticles; UV = ultraviolet.

3.2. Cell viability examination of MSCs

In addition, a cell viability test revealed that the population of MSCs was measured by a fluorescence microscope. In Figure 3A, after calcein-AM was hydrolyzed by esterases, calcein would be retained in cytoplasm and observed as a green colored fluorescence. The fluorescence intensity of calcein-AM was semiquantified after 48 hours of incubation and the results are indicated in Figure 3C. The fluorescence intensity was greatest in Chi-HA-Au 50 ppm (~1.98-fold, $p < 0.01$) group, compared with the Chi-HA-Au 25 ppm (~1.29-fold, $p < 0.01$) and Chi-HA (~0.62-fold) groups. Moreover, the marker for MSCs, CD44, was also investigated while culturing on different nanomaterials. The immunofluorescence staining of CD44 expression (Fig. 3B), as well as fluorescence intensity, was quantified at 1, 5, and 7 days (Fig. 3D). As Fig. 3D shows, the expression of CD44 in Chi-HA-Au 50 ppm at 1 day (~0.52-fold, $p < 0.05$) was higher than the Chi-HA-Au 25 ppm (~0.42-fold) and Chi-HA groups (~0.32-fold); and then at 5 days, the expression in Chi-HA-Au 50 ppm (~0.6-fold) was also greater than the other groups (Chi-HA-Au 25 ppm [~0.5-fold, $p < 0.05$] and Chi-HA [~0.49-fold, $p < 0.05$]). Finally, at the end of 7 days, the results concluded that while seeding MSCs on Chi-HA-Au 50 ppm (~0.69-fold, $p < 0.01$), the expression of CD44 was the highest, following by Chi-HA-Au 25 ppm (~0.62-fold, $p < 0.05$) and Chi-HA (~0.56-fold). The above evidence indicates that Chi-HA-Au 50 ppm could promote good survival and maintain the proliferation ability of MSCs. In brief, Chi-HA-Au 50 ppm may be a potential biomaterial for stem cell therapy.

3.3. Phenotype identification of MSCs

During this research, the immunophenotype of MSCs was examined by flow cytometry. Our team investigated the specific surface markers that were both positively and negatively relative to stem cells. The cells applied in this study were maintained within the eighth generation. The results indicate that MSCs did not express the differentiation markers of CD14, CD34, and CD45 which were belonging to the endothelial cells; and that the surface markers of CD29, CD44, and CD90 were observed, and were associated with the phenotype of human MSCs (Supplementary Fig. 1, http://links.lww.com/JCMA/A89).

3.4. Biocompatibility assay

Herein, the activation of monocytes was investigated. Monocytes (~5 μm) would accumulate and differentiate into macrophages (~40 to 45 μm), and then stimulate immune response. The semiquantification results of the number of monocytes and macrophages after incubating on various materials for 96 hours are shown in Fig. 4. In Fig. 4A, the number of monocytes was

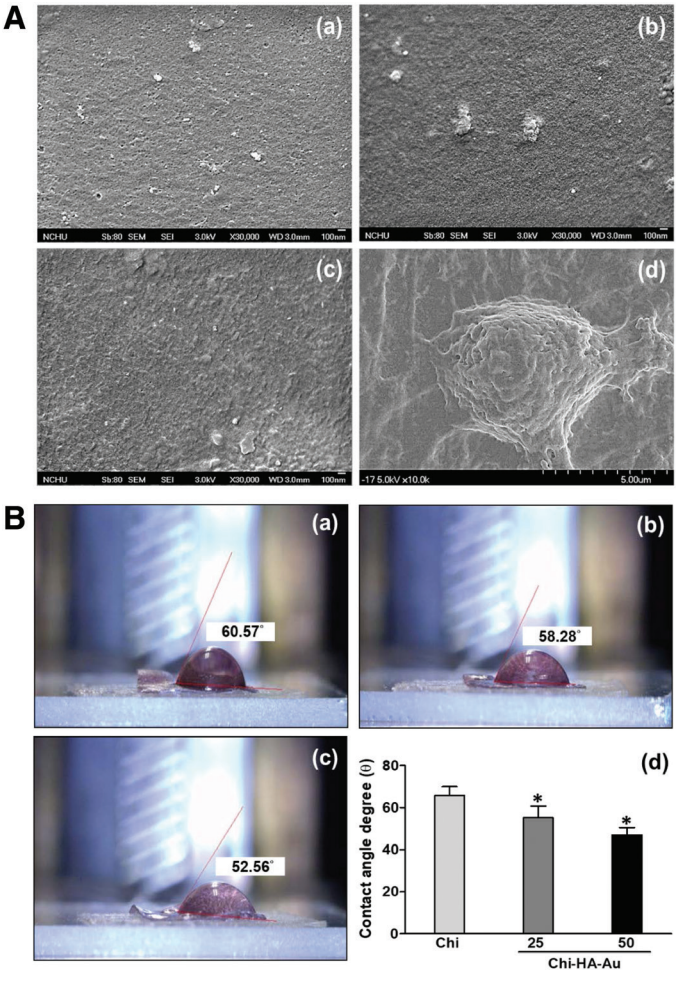

Fig. 2 SEM images showing the surface morphology of different materials. A, Control (TCPS), (b) Chi, (c) Chi-Au (25 ppm), and (d) Chi-Au (50 ppm). B, Contact angle test of various materials. The images of contact angle test in (a) Chi, (b) Chi-HA-Au 25 ppm, and (c) Chi-HA-Au 50 ppm. d, The average contact angle (θ) was quantified from different materials. The contact angle without water was θ = 0°. Data are the mean ± SD (n = 3). *$p < 0.05$, smaller than the Chi treatment. Au = gold; Chi = chitosan; HA = hyaluronic acid; TCPS = tissue culture polystyrene.

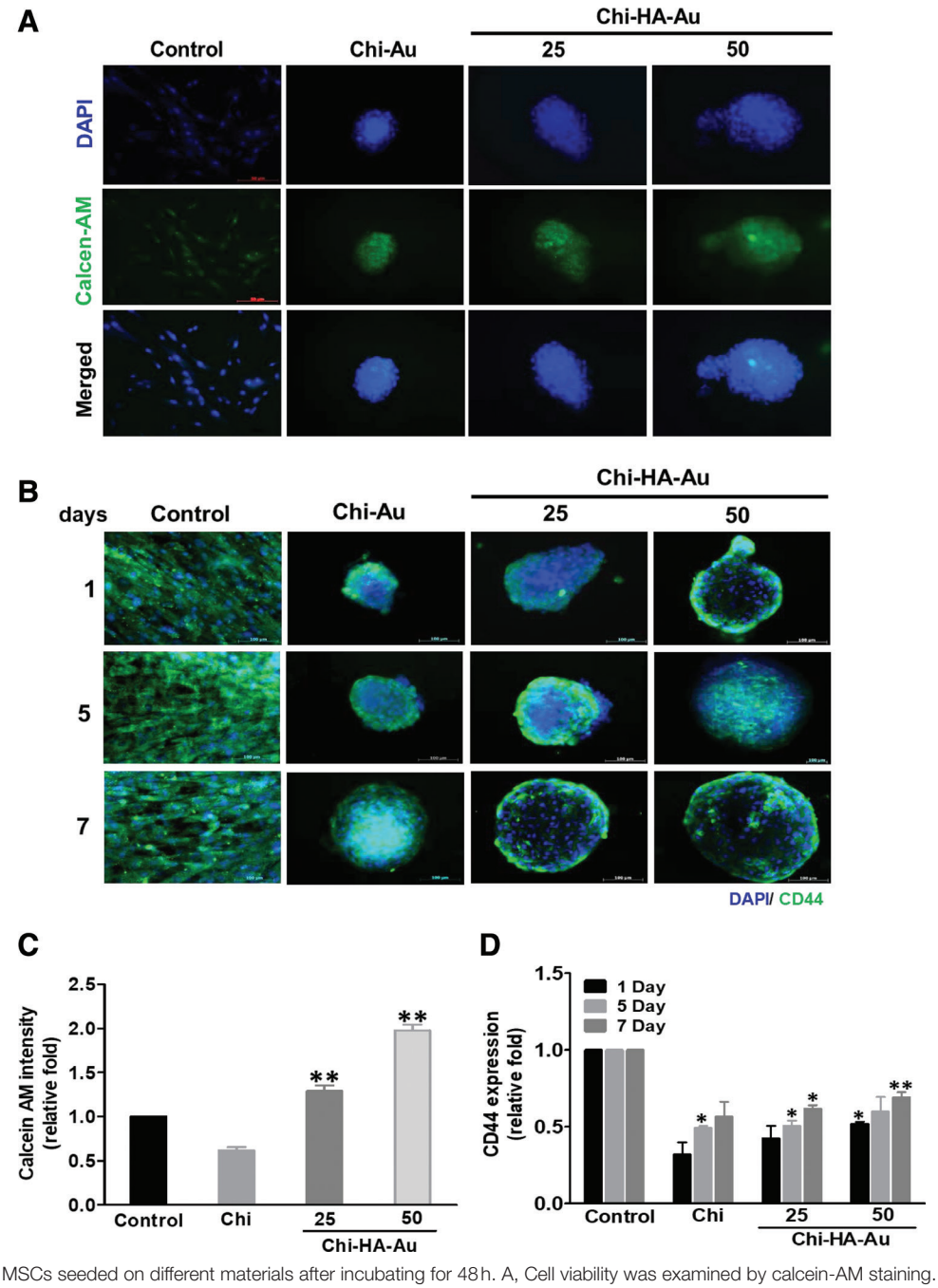

Fig. 3 Cell viability of MSCs seeded on different materials after incubating for 48 h. A, Cell viability was examined by calcein-AM staining. After calcein-AM was hydrolyzed by esterases, calcein would be retained in cytoplasm and could be measured (green color fluorescence). DAPI was used to stain cell nuclei (blue color fluorescence). Scale bar = 50 μm. The immunostaining of CD44 for MSCs culturing on various materials after 1, 5, and 7 d. B, The cells were immunostained by the primary anti-CD44 antibody and conjugated with the FITC-immunoglobulin secondary antibody (green color fluorescence). Cell nuclei was stained by DAPI (blue color fluorescence). Scale bar = 100 μm. C, The fluorescence intensity was quantified. $^{**}p < 0.01$: greater than the control (TCPS). D, CD 44 expression level was quantified based on fluorescence intensity. $^{*}p < 0.05$, $^{**}p < 0.01$: smaller than control (TCPS). AM = acetoxymethyl; DAPI = *4, 6-diamidino-2-phenylindole;* FITC = *fluorescein isothiocyanate;* MSC = mesenchymal stem cell; TCPS = tissue culture polystyrene.

greatly higher in the Chi-HA-Au 50 ppm (~21.7 × 10^4 cells, $p < 0.01$) and Chi-HA-Au 25 ppm (~21.5 × 10^4 cells, $p < 0.05$) groups, when compared with the control (~13 × 10^4 cells) and Chi-HA (~8.5 × 10^4 cells) groups. In contrast, Fig. 4B shows that the number of macrophages was significantly lower in the Chi-HA-Au 50 ppm (~0.5 × 10^4 cells, $p < 0.01$) group, followed by the Chi-HA-Au 25 ppm (~1.5 × 10^4 cells, $p < 0.05$), Chi-HA (~1.75 × 10^4 cells), and control (~1.75 × 10^4 cells) groups. Thus, as the conversion ratio indicates in Fig. 4C, the value of the Chi-HA-Au 50 ppm group was noticeably lower (~0.36-fold, $p < 0.01$) than the Chi-HA-Au 25 ppm (~0.63-fold, $p < 0.01$), Chi-HA (~1.77-fold), and control groups. The above results demonstrate that MSCs culturing on Chi-HA-AuNPs 50 ppm exhibited the least monocyte activation and conversion ratio, explaining that Chi-HA-AuNPs could promote anti-inflammatory ability and also provide better biocompatibility to help avoid foreign body reaction.

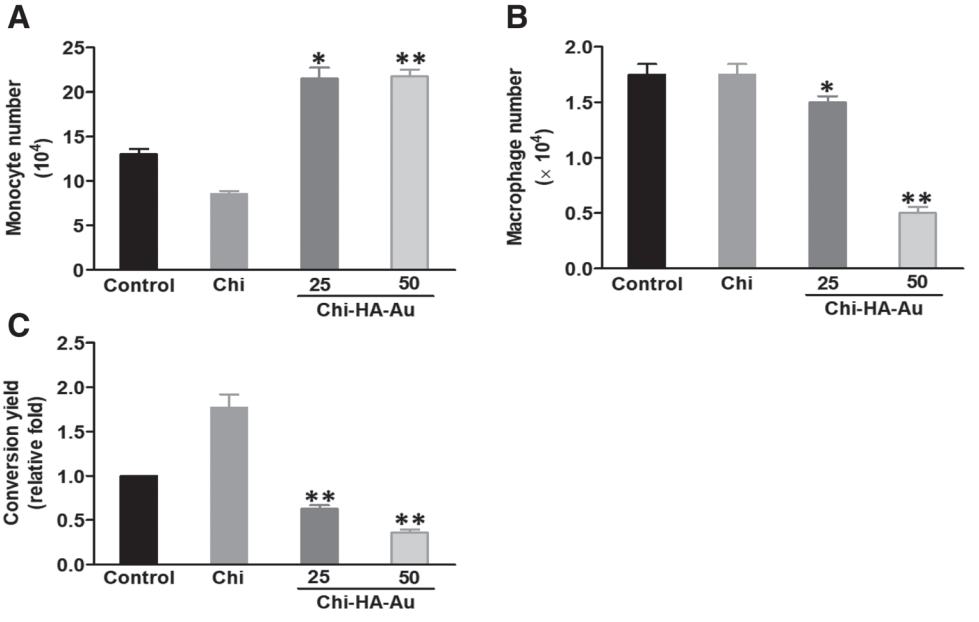

Fig. 4 Quantification of human monocytes and macrophages on different nanocomposites after 96 h of incubation. A, Number of monocytes. *$p < 0.05$; **$p < 0.01$: greater than the control (TCPS). B, Number of macrophages. *$p < 0.05$; **$p < 0.01$: smaller than the control (TCPS). C, Conversion ratio of monocytes transformed into macrophage. Data were the mean ± SD (n = 3). *$p < 0.05$; **$p < 0.01$: smaller than the control (TCPS). Au = gold; Chi = chitosan; HA = hyaluronic acid; TCPS = tissue culture polystyrene.

3.5. Colony formation ability of MSCs

To evaluate the cellular clonogenic potential of MSCs, colony formation assay was applied. The results are represented in Fig. 5. After seeding MSCs on different materials, the growth of MSCs at 1, 5, and 7 days was observed. Fig. 5A shows the growth condition through use of an optical microscope, with the semiquantification analysis represented in Fig. 5C. At day 1, the colony number of MSCs in Chi-HA-Au 50 ppm (~252.1 %, $p < 0.05$) was higher than that in both Chi-HA-Au 25 ppm (~178.1%) and Chi-HA (100%). Then, after growing for 5 days, the colony number of MSCs in the Chi-HA-Au 50 ppm group (~337.1%, $p < 0.01$) was also more than in the other two groups (Chi-HA-Au 25 ppm [~269.2%, $p < 0.05$], Chi-HA [~158.4%]). Finally, after incubating for 7 days, the colony number was greatest in the Chi-HA-Au 50 ppm group (~553.2%, $p < 0.05$), when compared with the Chi-HA-Au 25 ppm (~359.1%, $p < 0.01$) and Chi-HA (~252.4%) groups. Based on these results, Chi-HA-Au 50 ppm could induce MSCs to form more colonies. Since premature senescent cells are clonogenically inactive, it means that Chi-HA-Au could maintain stemness properties and strengthen cell viability.

To investigate the neurogenic differentiation activity of MSCs, the immunofluorescence staining of nestin (a neuroectodermal stem cell marker), β-tubulin (a neuron marker), and glial fibrillary acidic protein (GFAP; an astrocyte marker) were all analyzed with the results shown in Fig. 5B. Fig. 5B shows that the expression of nestin and β-tubulin in MSCs were the lowest while seeding on Chi-HA-Au 50 ppm, and that the shape of MSCs became more spherical after 48 hours incubating. Based on fluorescence intensity, the expression of nestin and GFAP was semiquantified and indicated in Fig. 5D. The nestin expression in MSCs on Chi-HA-Au 50 ppm was the lowest (~0.25-fold, $p < 0.05$), followed by Chi-HA-Au 25 ppm (~0.39-fold, $p < 0.05$) and Chi-HA (~0.54-fold, $p < 0.05$). Additionally, the expression of GFAP in the Chi-HA-Au 50 ppm group (~0.28-fold, $p < 0.01$) was also markedly less than the other groups (Chi-HA-Au 25 ppm [~0.45-fold, $p < 0.05$] and Chi-HA [~0.66-fold, $p < 0.05$]). Supplementary Fig. 2, http://links.lww.com/JCMA/A89, shows the semiquantification data of nestin and β-tubulin gene expression, which are similar to Fig. 5B. The above results indicate that Chi-HA-Au 50 ppm could control the expression of neural-related markers, as well as inhibiting neuron cell differentiation.

3.7. Gelatin zymography analysis

In Fig. 6, the MMP activity induced by Chi-HA-AuNPs was being examined by real-time PCR after incubating for 48 hours. Based on the results, the bands of Chi-HA-Au 50 ppm showed that both MMP-9 (90 KDa) and MMP-2 (62 KDa) displayed the most expression when compared with the other groups (Fig. 6A). The semiquantification of MMP2/9 gene expression is represented in Fig. 6B, C. Indeed, the MMP-2 expression in MSCs on Chi-HA-Au 50 ppm (~1.59-fold, $p < 0.01$) was higher than those in the Chi-HA-Au 25 ppm (~1.42-fold, $p < 0.01$) and Chi-HA (~1.12-fold) groups. MMP-9 expression was also the greatest in Chi-HA-Au 50 ppm (~1.12-fold, $p < 0.05$), followed by Chi-HA-Au 25 ppm (~1.1-fold, $p < 0.05$) and Chi-HA (~0.98-fold). These findings indicate that Chi-HA-Au 50 ppm may strengthen both angiogenesis and wound healing ability.

3.8. Biocompatibility examination in rat subcutaneous implantation

Indeed, chronic inflammation may lead to fibrosis, causing poor tissue regeneration and influencing the biocompatible capacity of biomaterials. Therefore, a successful implantation is usually determined by the interaction of cells and molecules between the implanted body and host tissue. Concerning fibrotic capsulation, the results of hematoxylin and eosin staining is shown in Fig. 7A. The semiquantification analysis results are represented in Fig. 7B, C. Here, the capsule thickness value was at its least in the Chi-HA-Au 50 ppm group (~0.48, $p < 0.01$), followed by the Chi-HA-Au 25 ppm (~0.65, $p < 0.01$) and Chi-HA groups (~0.9, $p < 0.05$). Moreover, the collagen deposition was also investigated

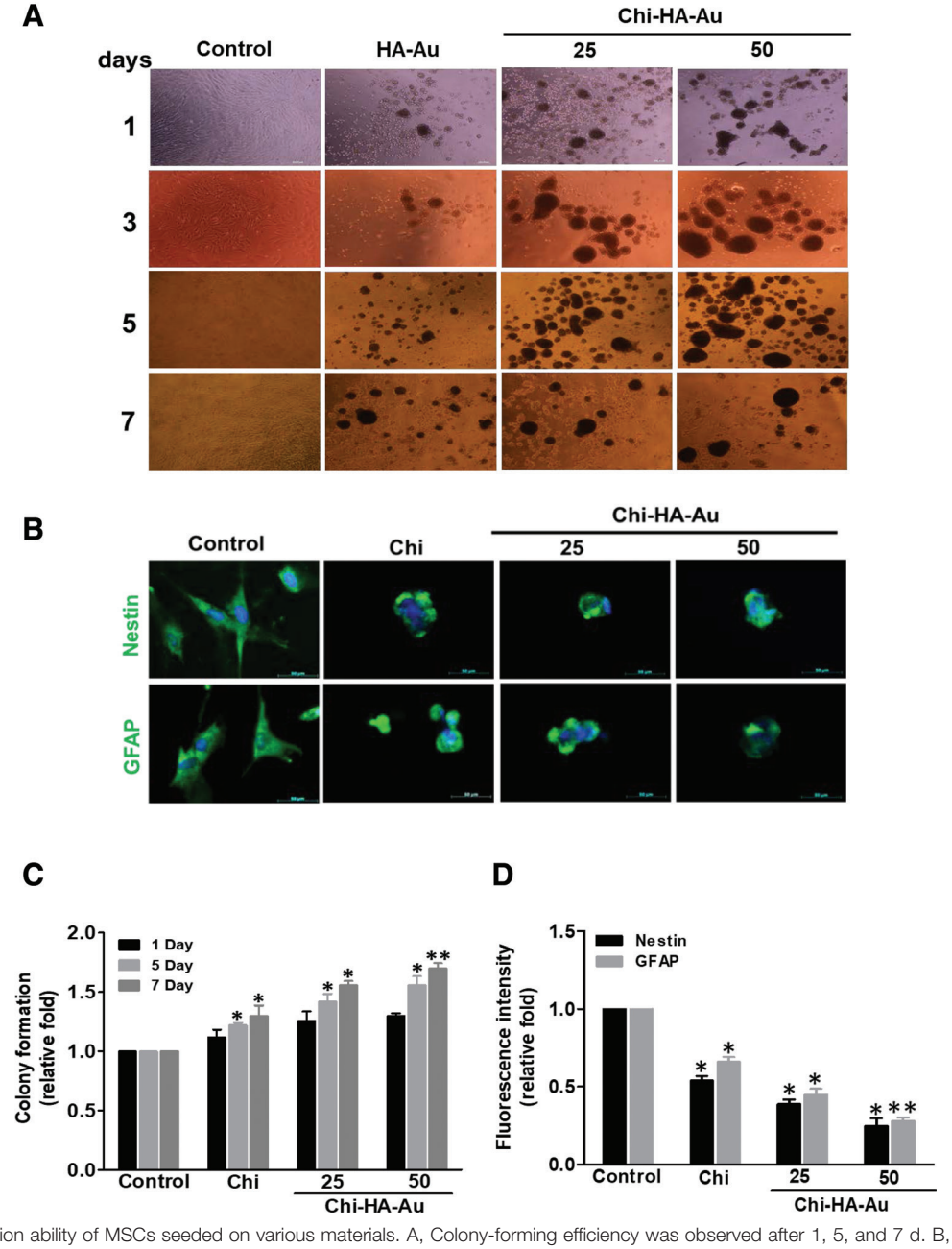

Fig. 5 Colony formation ability of MSCs seeded on various materials. A, Colony-forming efficiency was observed after 1, 5, and 7 d. B, Immunofluorescence staining of nestin and β-tubulin protein in MSCs seeded on various materials. After seeding on different materials for 48 h, the expression of nestin and β-tubulin antibodies (green color) was observed. Cell nuclei were stained by DAPI (blue color). Scale bar = 50 μm. C, Colony number was quantified based on percentage. The results represent the mean ± SD of three independent experiments. *$p < 0.05$; **$p < 0.01$: greater than the Chi-HA groups. D, Nestin and GFAP expression was quantified based on fluorescence intensity. *$p < 0.05$; **$p < 0.01$: smaller than the control (TCPS). Au = gold; Chi = chitosan; DAPI = *4, 6-diamidino-2-phenylindole; GFAP* = glial fibrillary acidic protein; HA = hyaluronic acid; MSC = mesenchymal stem cell; TCPS = tissue culture polystyrene.

through histologic examination, where the Chi-HA-Au 50 ppm group (~0.58, $p < 0.01$) was less than the other groups (Chi-HA-Au 25 ppm [~0.72, $p < 0.01$] and Chi-HA [~0.85, $p < 0.05$]).

3.9. Schematic illustrations

According to all of the above findings, Chi-HA-Au 50 ppm nanocomposites could induce CD44 and MMP expression, inhibit the expression of nestin, β-tubulin, and GFAP in vitro, and also modulate immune responses to provide better biocompatible properties in vivo. Our research team organized a summary illustration of Chi-HA-AuNPs (50 ppm) as a potential biomaterial for regulating the differentiation of MSCs in both neural repair and regeneration (Fig. 8).

4. DISCUSSION

As mentioned above, challenges still remain in creating suitable biomaterial for neural tissue engineering, including low toxicity, high biocompatibility, and effectiveness.[34] Though the biotechnology is being continuously developed in regenerative treatments, CNS damage such as SCI and Alzheimer's disease are difficult to overcome. This research indicates that the functional

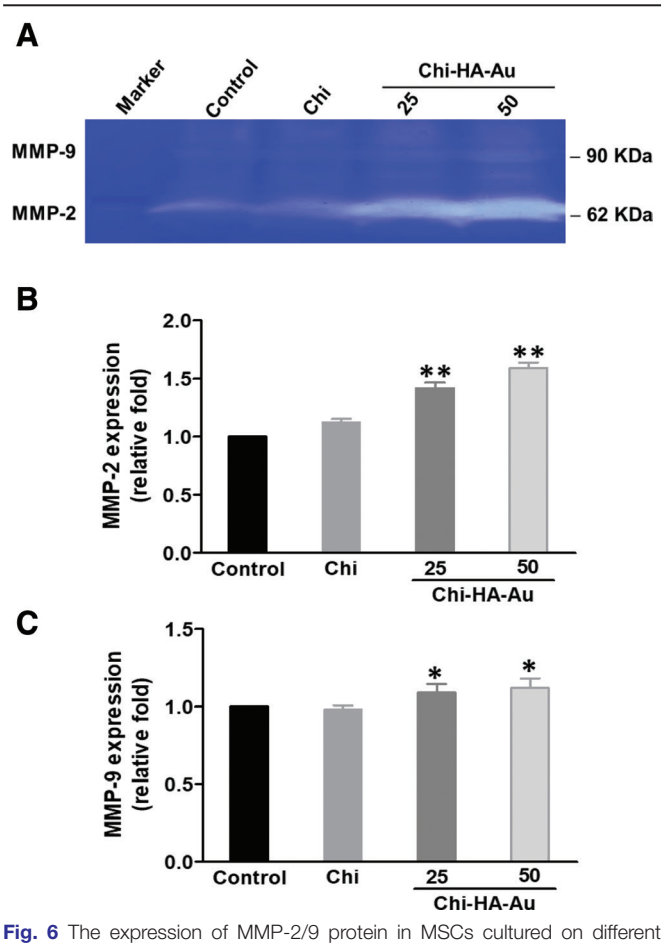

Fig. 6 The expression of MMP-2/9 protein in MSCs cultured on different materials for 48 h. A, The MMP-2/9 enzymatic activity of MSCs was increased in the Chi-HA-Au groups (~25 and 50 ppm). The semiquantitative measurement of (B) MMP-2 and (C) MMP-9 protein expression indicated that MSCs on Chi-HA-Au (25 and 50 ppm) had a significantly high level of expression. Data are presented as mean ± SD (n = 3). *$p < 0.05$; **$p < 0.01$: greater than the control (TCPS). Au = gold; Chi = chitosan; HA = hyaluronic acid; MMP = matrix metalloproteinase; MSC = mesenchymal stem cell; TCPS = tissue culture polystyrene.

biomaterials, Chi, HA, and collagen, are characterized as potential materials for CNS regeneration. In this study, Chi-HA-AuNP nanocomposites were employed to culture with MSCs. The evidence demonstrates that these kinds of nanocomposites could facilitate MSC survival rates and inhibit the expression of nestin and β-tubulin, as well as the guiding of neural cell differentiation. In addition, Chi-HA-AuNPs provided safety properties to help protect surrounding tissue while being implanted in our rat models. In short, the results reveal the potential of Chi-HA-AuNPs being cocultured with MSCs for neural tissue regeneration.

Previous studies have also investigated Chi-based scaffolds in nerve regeneration. The effects of valproic acid–labeled Chi Nps (VA-CN) on endogenous spinal cord NSCs were evaluated in rat models experiencing SCI. The results suggest that VA-CN could promote the proliferation of NSCs along with the expression of neurotrophic factors; and that VA-CN could also facilitate the Tuj 1–positive cells in the spinal cords of rats, as well as enhance the differentiation of NSCs.[35] Additional research shows there has been work being done on developing core-shell spheroids of NSCs and MSCs by coculturing cells on a Chi surface. This study reported that NSCs in Chi displayed a higher survival rate, and that the direct interaction of NSCs with MSCs facilitated both notch activity and differentiation capacity. Additionally, the differentiation ability of MSCs in Chi also promoted neural lineages. In a zebrafish model, study results have shown a higher survival rate in adult fish when implanted with Chi-derived NSC/MSC cospheroids. The above data suggest that Chi may provide an ECM-like environment and interaction between NSCs and MSCs to enhance neural differentiation abilities.[36] In addition, there was a study which focused on investigating water absorption, in vitro degradation, and the biocompatibility of Chi/gelatin porous scaffolds contained in HA and heparan sulfate (HS), while culturing with neural stem and PCs (NS/PCs). The results show that the Cs/Gel/HA/HS composite scaffolds were suitable for neural cell adhesion, survival, and growth.[37]

With regard to tissue engineering, an ideal biomaterial scaffold should have both perfect biocompatibility and mechanical properties, particularly for neural regeneration. AuNps are considered to possess the ability to manipulate the microstructure of a synthetic or natural polymer even in low concentrations.[29] The microstructural change of the polymer often improves biological functions. Additionally, the size of Nps may be crucial to their effects. Consequently, AuNPs (~5 nm) were used in this current research and expected to interact with Chi-HA. The evidence indicates that nanocomposites could become a better solution when constructing biomaterial scaffolds for neural repair.

When AuNPs are added in a polymer at the optimized concentration, a more favorable morphology is generated in the polymer.[27] A research study evaluated that AuNps at 25 or 50 ppm could lead to better cell performance for NSCs. The same study also discussed how the modification of Chi matrix by AuNPs can provide mechanical strength and affect cellular response.[38] Due to the small size of AuNPs, they are very effective in manipulating the interface of the composite; in other words, the amount of AuNPs required to change the microstructure may be low. Thus, a higher concentration of AuNPs may interfere with the microstructure and biological performance of the polymer.[39–41] In the current study, the characteristic dimensions of Chi-HA in the concentration of AuNPs 50 ppm was consistent with the favorable dimensions discussed in the available literature (100 nm). The contact angle test indicated that Chi-HA-Au 50 ppm offered better hydrophilicity properties for both cell attachment and surface morphological changes. The above results indicate that an optimized amount of AuNPs was important for the nanotopography specifics for Chi-HA and can be effective in guiding cells toward producing better attachment. Meanwhile, there have been many references which have proved that cells prefer to adhere to the hydrophilic surface of biomaterials. Therefore, the result of FTIR spectra suggests that there was interaction between Chi-HA and AuNPs.

The morphological change in the concentration of Chi-HA-Au 50 ppm increased cell viability, colony formation and maintained the stemness properties of MSCs. Additionally, the evidence reveals that Chi-HA-Au 50 ppm reduced inflammatory response compared with the control group. After culturing MSCs with Chi-HA-Au 50 ppm, the cell viability was better than in other groups. Meanwhile, we had also examined the marker of MSCs, CD44, and discovered that the expression level was higher than that seen in different concentrations of materials.[42] These findings indicate that AuNPs have the potential to improve biological performance. In conjunction, the results of colony formation concluded that Chi-HA-Au 50 ppm can induce more colony formation of MSCs, meaning the nanocomposites could maintain their stemness properties and cell viability. And when combined with the results of neural marker (nestin and β-tubulin) expression, it was possible to actually confirm that Chi-HA-Au 50 ppm can inhibit neuron cell differentiation. Currently, many studies are reporting that when stem cells are in the differentiation stage, the activation of MMP2/9 will be triggered and therefore

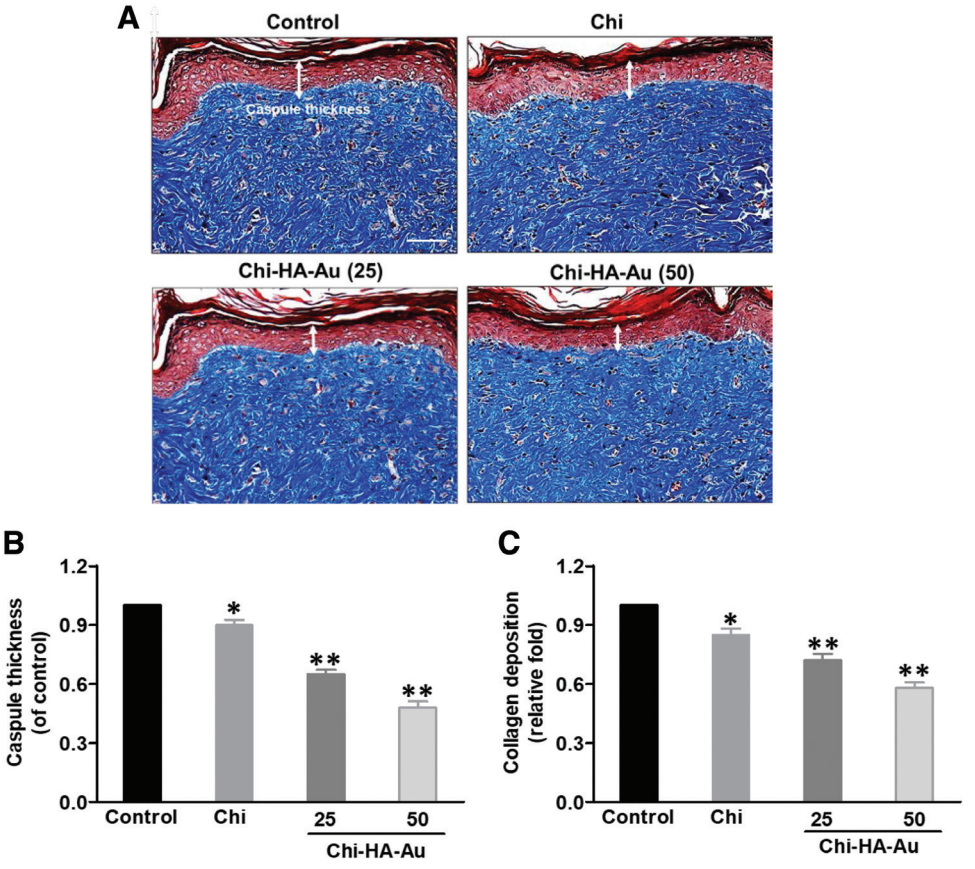

Fig. 7 Investigation of foreign body response in various materials after subcutaneous implantation. A, After 4 wk of implantation, histology of H&E staining was used to do the following quantification. Scale bar = 100 μm. B, Foreign body response was evaluated by the capsule thickness based on histology examination. *$p < 0.05$; **$p < 0.01$: less than the control (TCPS). C, Semiquantification of collagen deposition. *$p < 0.05$; **$p < 0.01$: smaller than the control (TCPS). Au = gold; Chi = chitosan; HA = hyaluronic acid; H&E = hematoxylin and eosin; TCPS = tissue culture polystyrene.

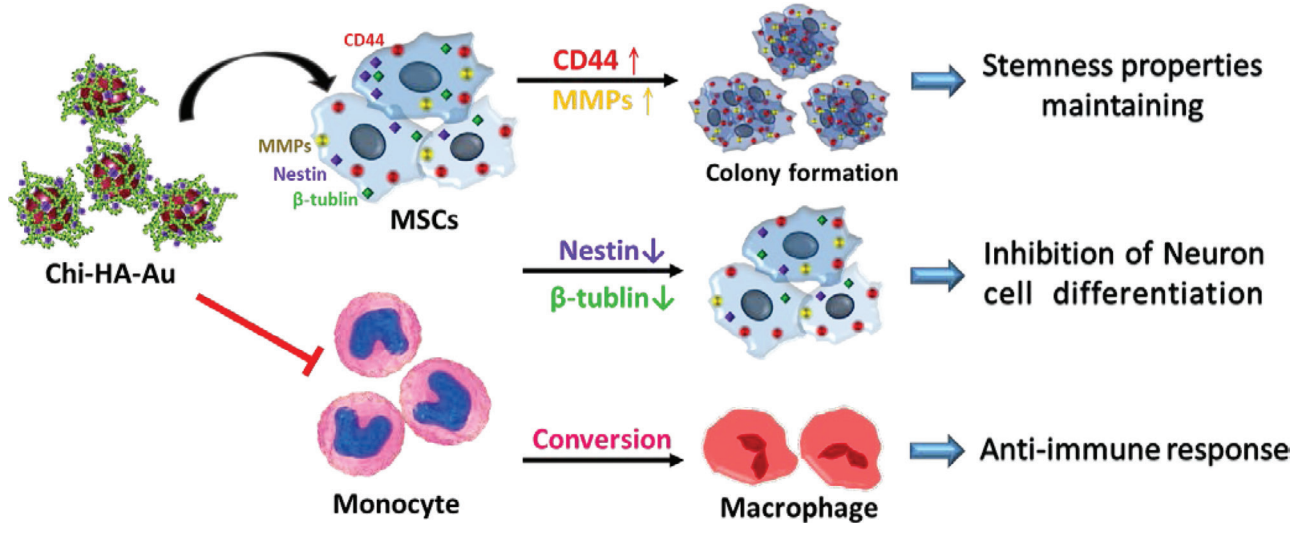

Fig. 8 Schematic illustrations. The diagram shows that Chi-HA-Au has the potential to inhibit differentiation and maintain colony formation of MSCs. Au = gold; Chi = chitosan; HA = hyaluronic acid; MMP = matrix metalloproteinase; MSC = mesenchymal stem cell.

effectively promote stem cells toward migration and differentiation.[43] As our results indicate, when we investigated the expression levels of MMP2/9, we discovered that Chi-HA-Au 50 ppm can stimulate MMP expression, when compared with other concentrations of materials.

MSCs are a fantastic cell source for tissue engineering due to their capacity for differentiation and secretion of bioactive factors that are immunomodulatory in their therapeutic potential.[44] In summary, this study suggests that the properties of Chi-HA nanobiomaterials can be modulated by making composites with AuNps, with these property changes inhibiting immune response. When looking toward formulating a medicine that can regulate the differentiation of MSCs and maintain the stemness properties, Chi-HA-Au nanocomposites may be a promising biomaterial for neural regeneration.

In conclusion, this research, our team created Chi-HA-AuNP nanocomposites (~25 and 50 ppm of AuNPs), with the attempt to realize their effects on the behavior of MSCs. The evidence indicates that Chi-HA-AuNPs could strengthen the cell viability of MSCs and maintain their stemness properties, particularly on 50 ppm of Chi-HA-Au. Moreover, after seeding MSCs in varying concentrations of Chi-HA-AuNP, the nanocomposites actually inhibited both the expression of neural-related markers (nestin and β-tubulin) and the activation of monocytes. MMP and CD44 (the marker of MSC) expression were also examined on being induced by Chi-HA-Au, with the results demonstrating that MMP2/9 and CD44 expression significantly increased when incubated with Chi-HA-AuNP 50 ppm in vitro. Furthermore, capsule formation and collagen deposition were also at the lowest after implanting Chi-HA-AuNP 50 ppm into our rat model. To sum up, according to the results surrounding cell viability, anti-immune response and inhibition of neural-related marker expression for MSCs grown on Chi-HA-AuNP nanocomposites, this type of nanofilm can provide appropriate applications for neural repair and regeneration engineering.

APPENDIX A. SUPPLEMENTARY DATA

Supplementary data related to this article can be found at http://links.lww.com/JCMA/A89.

REFERENCES

1. Kim H, Cooke MJ, Shoichet MS. Creating permissive microenvironments for stem cell transplantation into the central nervous system. *Trends Biotechnol* 2012;**30**:55–63.
2. Martino S, D'Angelo F, Armentano I, Kenny JM, Orlacchio A. Stem cell-biomaterial interactions for regenerative medicine. *Biotechnol Adv* 2012;**30**:338–51.
3. Mothe AJ, Tator CH. Review of transplantation of neural stem/progenitor cells for spinal cord injury. *Int J Dev Neurosci* 2013;**31**:701–13.
4. Kim SU, Lee HJ, Kim YB. Neural stem cell-based treatment for neurodegenerative diseases. *Neuropathology* 2013;**33**:491–504.
5. Bühnemann C, Scholz A, Bernreuther C, Malik CY, Braun H, Schachner M, et al. Neuronal differentiation of transplanted embryonic stem cell-derived precursors in stroke lesions of adult rats. *Brain* 2006;**129**(Pt 12):3238–48.
6. Amariglio N, Hirshberg A, Scheithauer BW, Cohen Y, Loewenthal R, Trakhtenbrot L, et al. Donor-derived brain tumor following neural stem cell transplantation in an ataxia telangiectasia patient. *PLoS Med* 2009;**6**:e1000029.
7. Roffi A, Nakamura N, Sanchez M, Cucchiarini M, Filardo G. Injectable systems for intra-articular delivery of mesenchymal stromal cells for cartilage treatment: a systematic review of preclinical and clinical evidence. *Int J Mol Sci* 2018;**19**:E3322.
8. Kim DW, Staples M, Shinozuka K, Pantcheva P, Kang SD, Borlongan CV. Wharton's jelly-derived mesenchymal stem cells: phenotypic characterization and optimizing their therapeutic potential for clinical applications. *Int J Mol Sci* 2013;**14**:11692–712.
9. Yan Y, Ma T, Gong K, Ao Q, Zhang X, Gong Y. Adipose-derived mesenchymal stem cell transplantation promotes adult neurogenesis in the brains of Alzheimer's disease mice. *Neural Regen Res* 2014;**9**:798–805.
10. Yang E, Liu N, Tang Y, Hu Y, Zhang P, Pan C, et al. Generation of neurospheres from human adipose-derived stem cells. *Biomed Res Int* 2015;**2015**:743714.
11. Thein-Han WW, Misra RD. Biomimetic chitosan-nanohydroxyapatite composite scaffolds for bone tissue engineering. *Acta Biomater* 2009;**5**:1182–97.
12. Oyarzun-Ampuero FA, Brea J, Loza MI, Torres D, Alonso MJ. Chitosan-hyaluronic acid nanoparticles loaded with heparin for the treatment of asthma. *Int J Pharm* 2009;**381**:122–9.
13. Wang G, Lu G, Ao Q, Gong Y, Zhang X. Preparation of cross-linked carboxymethyl chitosan for repairing sciatic nerve injury in rats. *Biotechnol Lett* 2010;**32**:59–66.
14. Croisier F, Jérôme C. Chitosan-based biomaterials for tissue engineering. *Eur Polym J* 2013;**49**:780–92.
15. Skop NB, Calderon F, Levison SW, Gandhi CD, Cho CH. Heparin crosslinked chitosan microspheres for the delivery of neural stem cells and growth factors for central nervous system repair. *Acta Biomater* 2013;**9**:6834–43.
16. Lutolf MP, Gilbert PM, Blau HM. Designing materials to direct stem-cell fate. *Nature* 2009;**462**:433–41.
17. Jha AK, Xu X, Duncan RL, Jia X. Controlling the adhesion and differentiation of mesenchymal stem cells using hyaluronic acid-based, doubly crosslinked networks. *Biomaterials* 2011;**32**:2466–78.
18. Tang S, Vickers SM, Hsu HP, Spector M. Fabrication and characterization of porous hyaluronic acid-collagen composite scaffolds. *J Biomed Mater Res A* 2007;**82**:323–35.
19. Yamane S, Iwasaki N, Kasahara Y, Harada K, Majima T, Monde K, et al. Effect of pore size on in vitro cartilage formation using chitosan-based hyaluronic acid hybrid polymer fibers. *J Biomed Mater Res A* 2007;**81**:586–93.
20. Yun YH, Goetz DJ, Yellen P, Chen W. Hyaluronan microspheres for sustained gene delivery and site-specific targeting. *Biomaterials* 2004;**25**:147–57.
21. Zheng Shu X, Liu Y, Palumbo FS, Luo Y, Prestwich GD. In situ crosslinkable hyaluronan hydrogels for tissue engineering. *Biomaterials* 2004;**25**:1339–48.
22. Carvalho MP, Costa EC, Miguel SP, Correia IJ. Tumor spheroid assembly on hyaluronic acid-based structures: a review. *Carbohydr Polym* 2016;**150**:139–48.
23. Collins MN, Birkinshaw C. Hyaluronic acid based scaffolds for tissue engineering—a review. *J Carbonhydr Polym* 2013;**92**:1262–79.
24. Tang Z, Wang Y, Podsiadlo P, Kotov N. Biomedical applications of layer-by-layer assembly: from biomimetics to tissue engineering. *J Adv Mater* 2006;**18**:3203–24.
25. Yadid M, Feiner R, Dvir T. Gold nanoparticle-integrated scaffolds for tissue engineering and regenerative medicine. *Nano Lett* 2019;**19**:2198–206.
26. Nimi N, Paul W, Sharma CP. Blood protein adsorption and compatibility studies of gold nanoparticles. *J Gold Bull* 2011;**44**:15–20.
27. Chou CW, Hsu SH, Wang PH. Biostability and biocompatibility of poly(ether)urethane containing gold or silver nanoparticles in a porcine model. *J Biomed Mater Res A* 2008;**84**:785–94.
28. Hsu SH, Tang CM, Tseng HJ. Biostability and biocompatibility of poly (ester urethane)–gold nanocomposites. *J Acta Biomaterialia* 2008;**4**:1797–808.
29. Hung HS, Tang CM, Lin CH, Lin SZ, Chu MY, Sun WS, et al. Biocompatibility and favorable response of mesenchymal stem cells on fibronectin-gold nanocomposites. *PLoS One* 2013;**8**:e65738.
30. Hung HS, Chang CH, Chang CJ, Tang CM, Kao WC, Lin SZ, et al. In vitro study of a novel nanogold-collagen composite to enhance the mesenchymal stem cell behavior for vascular regeneration. *PLoS One* 2014;**9**:e104019.
31. Yen HJ, Hsu SH, Tsai CL. Cytotoxicity and immunological response of gold and silver nanoparticles of different sizes. *Small* 2009;**5**:1553–61.
32. Goldstein JI, Newbury DE, Michael JR, Ritchie NW, Scott JHJ, Joy DC. Scanning electron microscopy and X-ray microanalysis. Springer; 2017.
33. Franken NA, Rodermond HM, Stap J, Haveman J, van Bree C. Clonogenic assay of cells in vitro. *Nat Protoc* 2006;**1**:2315–9.
34. Couet F, Rajan N, Mantovani D. Macromolecular biomaterials for scaffold-based vascular tissue engineering. *Macromol Biosci* 2007;**7**:701–18.

35. Wang D, Wang K, Liu Z, Wang Z, Wu H. Valproic acid labeled chitosan nanoparticles promote the proliferation and differentiation of neural stem cells after spinal cord Injury. *Neurotox Res* 2021;**39**:456–66.
36. Han HW, Hsu SH. Chitosan derived co-spheroids of neural stem cells and mesenchymal stem cells for neural regeneration. *Colloids Surf B Biointerfaces* 2017;**158**:527–38.
37. Guan S, Zhang XL, Lin XM, Liu TQ, Ma XH, Cui ZF. Chitosan/gelatin porous scaffolds containing hyaluronic acid and heparan sulfate for neural tissue engineering. *J Biomater Sci Polym Ed* 2013;**24**:999–1014.
38. Lin YL, Jen JC, Hsu SH, Chiu IM. Sciatic nerve repair by microgrooved nerve conduits made of chitosan-gold nanocomposites. *Surg Neurol* 2008;**70**(Suppl 1):S1:9–18.
39. Huang CY, Lin CH, Ho TT, Chen HC, Chu MY, Sun WS, et al. Enhanced migration of Wharton's jelly mesenchymal stem cells grown on polyurethane nanocomposites. *JMBE* 2013;**33**:139–48.
40. Hung HS, Chu MY, Lin CH, Wu CC, Hsu SH. Mediation of the migration of endothelial cells and fibroblasts on polyurethane nanocomposites by the activation of integrin-focal adhesion kinase signaling. *J Biomed Mater Res A* 2012;**100**:26–37.
41. Hung HS, Hsu SH. The response of endothelial cells to polymer surface composed of nanometric micelles. *N Biotechnol* 2009;**25**:235–43.
42. Zhu H, Mitsuhashi N, Klein A, Barsky LW, Weinberg K, Barr ML, et al. The role of the hyaluronan receptor CD44 in mesenchymal stem cell migration in the extracellular matrix. *Stem Cells* 2006;**24**:928–35.
43. Zhang H, Zhu T, Zhang L, Wu Q. Stromal cell-derived factor-1 induces matrix metalloproteinase expression in human endplate chondrocytes, cartilage endplate degradation in explant culture, and the amelioration of nucleus pulposus degeneration in vivo. *Int J Mol Med* 2018;**41**:969–76.
44. Caplan AI, Dennis JE. Mesenchymal stem cells as trophic mediators. *J Cell Biochem* 2006;**98**:1076–84.